Article

Reactive Distillation for Two-Stage Reaction Systems: Adipic Acid and Glutaric Acid Esterifications

Shih-Bo Hung, I-Kuan Lai, Hsiao-Ping Huang, Ming-Jer Lee, and Cheng-Ching Yu

More About This Article

Additional resources and features associated with this article are available within the HTML version:

- Supporting Information
- Access to high resolution figures
- Links to articles and content related to this article
- Copyright permission to reproduce figures and/or text from this article

View the Full Text HTML

ACS Publications
High quality. High impact.

Reactive Distillation for Two-Stage Reaction Systems: Adipic Acid and Glutaric Acid Esterifications

Shih-Bo Hung,[†] I-Kuan Lai,[‡] Hsiao-Ping Huang,[‡] Ming-Jer Lee,[†] and Cheng-Ching Yu*,[‡]

Departments of Chemical Engineering, National Taiwan University, Taipei 106-17, Taiwan, and National Taiwan University of Science and Technology, Taipei 106-07, Taiwan

Two new complete reactive distillation processes for two-stage reaction systems (adipic acid and glutaric acid esterifications with methanol) are explored. Similarities and differences between these two flowsheets have been identified. Both the diacid esterification reactions are catalyzed heterogeneously by an acidic ion-exchange resin, and reaction kinetics can be described using quasihomogeneous model. The UNIFAC method predicts suitable NRTL parameters for calculating liquid activity coefficients, which give a good description of experimental data. Results show that the plantwide flowsheets need a large recycle ratio for the light key reactants and ester products could be achieved with a purity of 99 mol %. A systematic design procedure for the complete flowsheets is presented, and the optimum operating conditions of the overall systems are studied to minimize the total annual cost while meeting the product specifications.

1. Introduction

Reactive distillation (RD) combines reaction and separation in a single unit and provides substantial economic benefit for some chemical processes. RD provides an attractive alternative for process intensification, especially for reaction/separation systems with reversible reactions. The books by Doherty and Malone[1] and Sundmacher and Kienle[2] give updated summaries of the field. Taylor and Krishna[3] describe potential advantages, modeling, simulation, and hardware configurations of reactive distillation. In the book by Sundmacher and Kienle,[2] there is a comprehensive list of the reactions that have been investigated as candidates for RD. According to the list collected, we may find that most of the industrial applications of RD may be divided into three reaction types: (A) simple reversible reaction, (B) parallel reactions, and (C) two-stage cascade reactions.

Type A and type B are two more common types applied in that the main applications for RD processes are etherification and esterification. A significant portion of the literature is devoted to esterification of acetic acid processes for which the reaction can be simply described as acid + alcohol ↔ acetate + water.[4–7] Although the reaction mechanism seems to be quite simple, the process design varies greatly for the different cases. Tang[8] et al. explored the applicable reactive distillation configurations for acetic acid esterification with different alcohols (ranging from C1 to C5) and provided systematic design procedures. The etherification is a notable example that is representative of type B, such as the production of MTBE or TAME.[9,10] Both reactions can be described as methanol + iso-olefin (isobutene/isoamylene) ↔ tert-ether (MTBE/TAME) and usually carried out in the presence of impurity for side reactions (1-butene in MTBE and n-pentene in TAME). Only a limited number of papers discuss the two-stage (type C) reaction in RD systems. A typical example is the reaction with the following form: A + B ↔ C + D, B + C ↔ D + E). Ung and Doherty[11,12] identified the feasible regions of product compositions for this type on the basis of phase and reaction equilibria. Luo and Xiao[13] studied the transesterification of dimethyl carbonate (DMC) and ethanol with methyl ethyl carbonate as an intermediate and the performance of different reactive distillation designs using rigorous steady-state simulation. There is another esterification type belonging to type C that has received little attention so far: a two-stage cascade esterification. An example follows: If a diacid is esterified with a monoalcohol, a monoester will be produced at the first stage and will simultaneously react with the alcohol to form a diester.

In this work, we explore two alternative RD flowsheets for diacid esterification processes. The conceptual design is based on the physical and thermodynamic properties of the system, and total annual cost (TAC) is used to evaluate the appropriateness of different designs. We use dimethyl adipate as the primary case study illustration, and compare it with dimethyl glutarate in section 6. Dimethyl adipate (DMA) is used as part of a dibasic ester (DBE) blend that is used as a major ingredient in several paint strippers. The DMA content in DBE blends varies from about 15% to 90%. The other components of the DBE blends are dimethyl glutarate (DMG) and dimethyl succinate (DMS). It is worthwhile to note that DBE has the advantages of very low toxicity, great stability, rather high boiling point, and viscosity and density that are close to water.

The paper is organized as follows. Section 2 describes the reaction kinetics of the adipic acid esterification. The physical properties and thermodynamic behaviors of DMA system are explored in section 3. On the basis of the thermodynamic analyses, two possible flowsheets are generated, and improved designs are sought by minimizing the TAC. Next, comparisons between these two flowsheets are made. Section 6 extends the design to dimethyl glutarate production. In this work, the design is carried out using Aspen Plus.
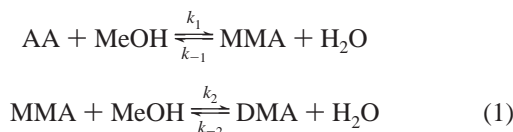
2. Reaction Kinetics

The esterification of adipic acid (AA) and methanol (MeOH) proceeds by two reversible cascade reactions with adipic acid monomethyl ester (monomethyl adipate, MMA) as an intermediate:

---

* Corresponding author. Tel.: +886-2-3366-3037. Fax: +886-2-2362-3040. E-mail: ccyu@ntu.edu.tw.

† National Taiwan University of Science and Technology.

‡ National Taiwan University.

$$AA + MeOH \underset{k_{-1}}{\overset{k_1}{\rightleftharpoons}} MMA + H_2O$$

$$MMA + MeOH \underset{k_{-2}}{\overset{k_2}{\rightleftharpoons}} DMA + H_2O \qquad (1)$$

The kinetics data and rate expressions are taken from the experimental work of Chan.[14] In Chan's work, Amberlyst 15 (Rohm and Hass) acidic ion-exchange resin was used as a solid catalyst, and quasihomogeneous models could quite appropriately describe the reaction mechanisms. The reaction rate expressions are as follows:

$$\frac{-dC_{AA}}{dt} = k_1 C_{AA} C_{MeOH} - k_{-1} C_{MMA} C_{H_2O}$$

$$\frac{-dC_{MeOH}}{dt} = k_1 C_{AA} C_{MeOH} - k_{-1} C_{MMA} C_{H_2O} + \\ k_2 C_{MMA} C_{MeOH} - k_{-2} C_{DMA} C_{H_2O}$$

$$\frac{dC_{MMA}}{dt} = k_1 C_{AA} C_{MeOH} - k_{-1} C_{MMA} C_{H_2O} - \\ k_2 C_{MMA} C_{MeOH} + k_{-2} C_{DMA} C_{H_2O}$$

$$\frac{dC_{H_2O}}{dt} = k_1 C_{AA} C_{MeOH} - k_{-1} C_{MMA} C_{H_2O} + \\ k_2 C_{MMA} C_{MeOH} - k_{-2} C_{DMA} C_{H_2O}$$

$$\frac{dC_{DMA}}{dt} = k_2 C_{MMA} C_{MeOH} - k_{-2} C_{DMA} C_{H_2O} \qquad (2)$$

where C_i represents the molar concentrations (mol/cm^3) of component i, and the forward reaction rate constants (cm^6/g cat/min/mol) can be expressed as

$$k_1 = 5.857 \times 10^6 \exp\left(\frac{-4097.8}{T}\right) \qquad (3)$$

$$k_2 = 2.024 \times 10^6 \exp\left(\frac{-4201.1}{T}\right) \qquad (4)$$

Because of negligible heat effects, the equilibrium constants are regarded as temperature independent; thus, we have

$$K_{1eq} = \frac{k_1}{k_{-1}} = 0.997 \qquad (5)$$

$$K_{2eq} = \frac{k_2}{k_{-2}} = 2.56 \qquad (6)$$

In applying the reaction kinetics to reactive distillation, it is assumed that the solid catalyst occupies 50% of the tray holdup volume and a catalyst density of 800 kg/m^3 is used to convert the volume into catalyst weight (m_{cat}).

3. Thermodynamics

3.1. Vapor Pressure. Aspen Plus has a built-in data bank with the pure components properties for water, MeOH, and AA, but it lacks data for the two esters, dimethyl adipate and monomethyl adipate. DMA and MMA have very low volatility; thus, the boiling point data are only available under very low pressure from the following data bank: NIST Chemistry WebBook June 2005 Release, http://webbook.nist.gov/chemistry/. In order to obtain the correct saturated vapor pressures of DMA, we take the experimental data[15] and make new correla-

tions. However, MMA has an even lower vapor pressure than DMA, and it is difficult to obtain reliable data for correlation. Therefore, we use MMA's Antonie coefficients of DECHEMA (http://www.dechema.de/). The extended Antoine equation is used, and parameters are given in appendix A. On the basis of vapor pressure models, we have the following normal boiling point ranking for these five components:

$$AA\ (337.47\ °C) > MMA\ (261.76\ °C) > \\ DMA\ (235.68\ °C) > H_2O\ (100.0\ °C) > \\ MeOH\ (64.53\ °C) \qquad (7)$$

Unfortunately, the two products (DMA and H$_2$O) are intermediate boilers whereas the reactants are the lowest and highest boilers, respectively. This is the worst case scenario for a reactive distillation.

3.2. Phase Equilibrium. The NRTL-HOC thermodynamic model is used to describe vapor−liquid equilibrium with liquid activity coefficients calculated by the nonrandom two-liquid (NRTL) model, and the vapor association was determined using the method of Hayden and O'Connel[16] (HOC). The Aspen Plus built-in parameters are employed to compute fugacity coefficients. For activity coefficient, H$_2$O−MeOH is the only pair that has the built-in parameter in Aspen Plus. The UNIFAC[17] group contribution method is used to estimate the remaining parameters. The predicted results are also verified with the experimental data.[15] The results show that the estimated parameters give reasonable predictions. Figure 1 shows the VLE (X−Y diagram) for all ten binary pairs. Figure 1a indicated that the relative volatility between AA and MeOH is quite large, and that implies it will be difficult to achieve good liquid−liquid contact between AA and MeOH. Since the reaction is carried out in the liquid phase, the "neat" (that is, no excess reactant) flowsheet is impossible. Methanol must be in great excess to ensure adequate liquid contact. For liquid−liquid equilibrium (LLE) calculation, in order to obtain improved accuracy, the NRTL parameter set[18] is used. The residue curve maps and the liquid−liquid envelopes for all ternary subsystems are shown in Figure 2. There exists a large two-liquid region, e.g., Figure 2c, that can be used for liquid−liquid separation. On the basis of the UNIFAC estimation, the system has only one binary azeotrope (water/DMA, 98.94/1.06 mol %), at a temperature of 99.77 °C. The azeotrope also locates in a two-phase zone, and more importantly, it corresponds to almost pure water. Since the azeotrope is predicted from estimated parameters, regardless of its existence, high purity water can be obtained via liquid−liquid separation. Appendix A gives all parameters for the vapor pressure and VLE and LLE correlations. The conceptual design will be explored next.

4. Process Flowsheet and Steady-State Design

4.1. Possible Configurations of Reactive Distillation Column (RDC). According to the normal boiling point ranking (eq 7), the products, DMA and water, are intermediate boilers, while the two reactants are the lightest (MeOH) and heaviest (AA) components. Thus, the removal of the products can be a problem, and the drastically different boiling points of the reactants make the liquid−liquid contact difficult. This implies that one-pass conversion can be very small. Tung and Yu[19] discuss the effects of relative volatility ranking on the design of reactive distillation columns. They treated the ideal quaternary system with reversible reaction, A + B ↔ C + D, and explored optimal flowsheet design based on the total annual cost (TAC). In one of the types they identified, type I$_r$, LLK + HHK = LK
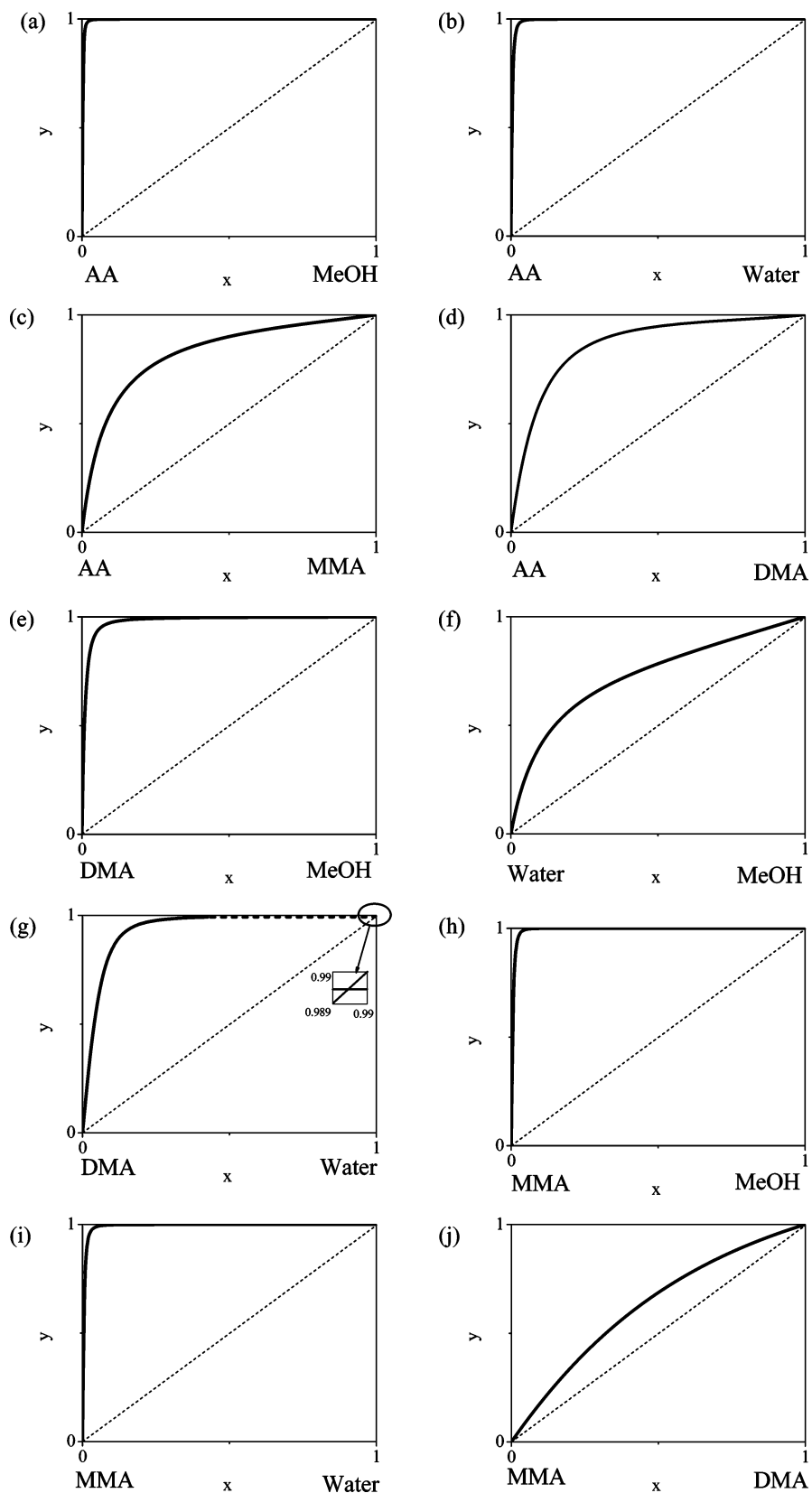
Figure 1. VLE diagrams for (a) adipic acid + methanol, (b) adipic acid + water, (c) adipic acid + monomethyl adipate, (d) adipic acid + dimethyl adipate, (e) dimethyl adipate + methanol, (f) water + methanol, (g) dimethyl adipate + water, (h) monomethyl adipate + methanol, (i) monomethyl adipate + water, and (j) monomethyl adipate + dimethyl adipate.

+ HK, which means the two reactants are lighter than light key component (LLK) A and heavier than heavy key component (HHK) B with the two products being light key component (LK) C and heavy key component (HK) D. According to the possible RDC configuration of this type by Tung and Yu,[19] the reactive

zones are placed at the opposite ends of the column where significant amounts of LLK and HHK (two reactants) are present (Figure 3, left part). The fresh heavy reactant (HHK) is introduced into the top of the column where a significant amount of the other reactant (LLK) is most abundant. Similarly, the
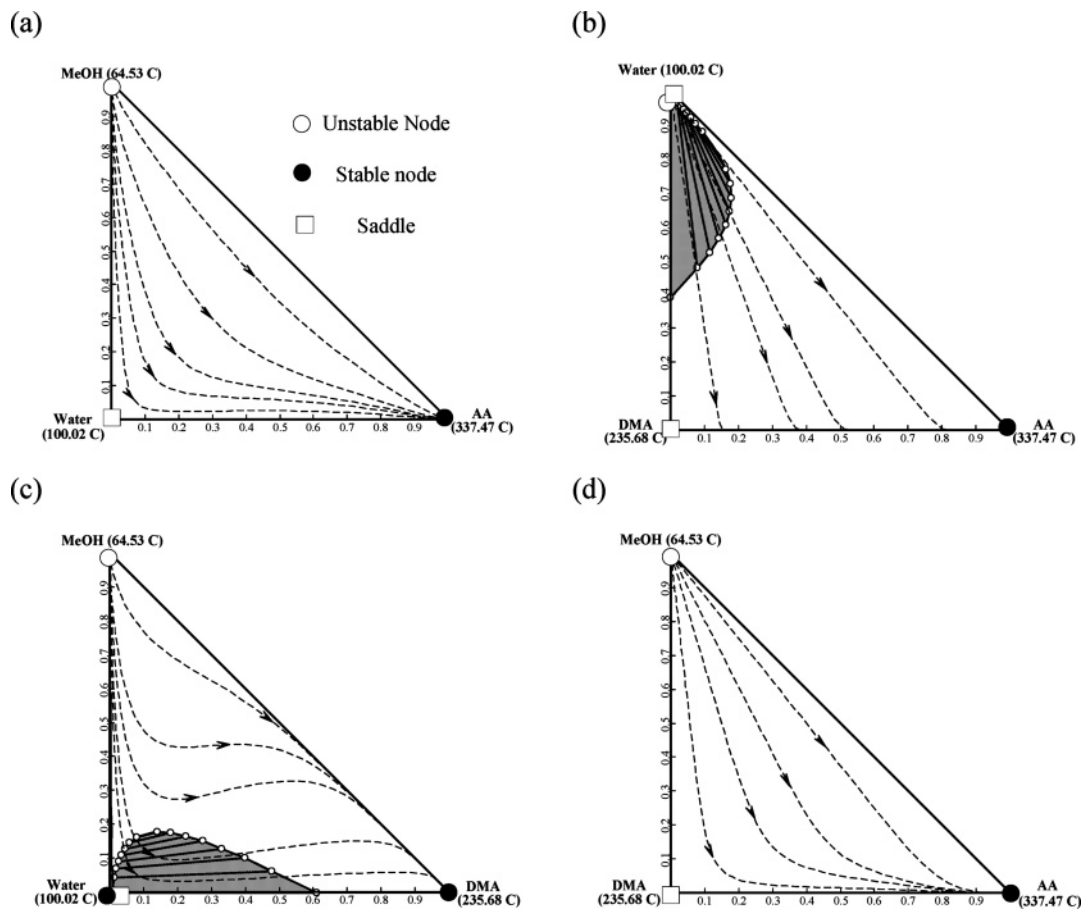
(a)

(b)

(c)

(d)

Figure 2. Ternary residual curve maps and two-liquid zone for methanol, adipic acid, dimethyl adipate, and water system at $P = 1$ atm.
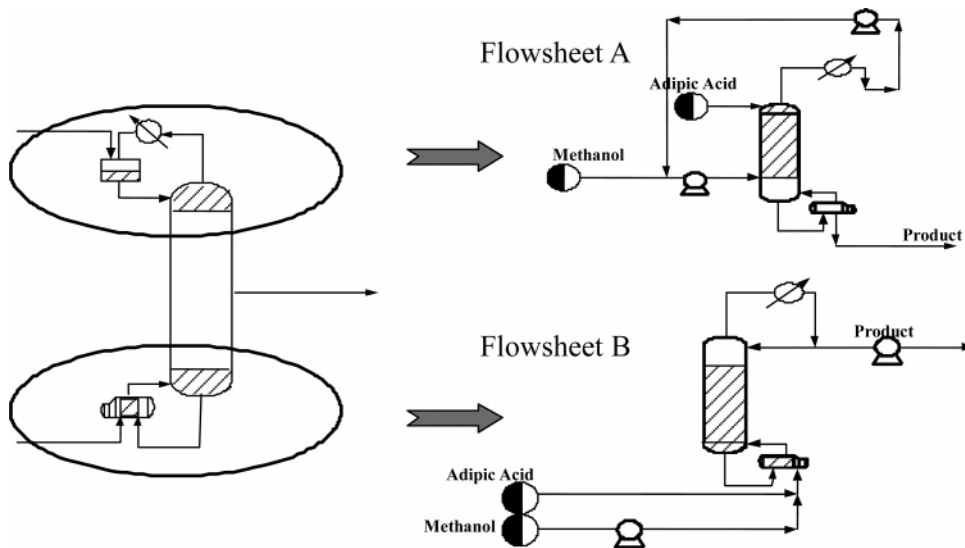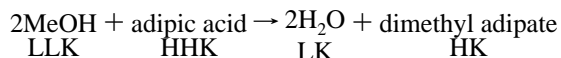

Figure 3. Two alternative reactive distillation configurations for excess reactant design.

fresh light reactant (LLK) is fed to the bottom of the column, where a significant amount of the heavy reactant (HHK) is present. Products are withdrawn from the midsection of the column as a side stream, and a product column is used to separate these two products. Considering the net adipic acid esterification, it also can be expressed as

$$2\text{MeOH} + \text{adipic acid} \rightarrow 2\text{H}_2\text{O} + \text{dimethyl adipate}$$
$$\quad\;\text{LLK} \qquad \text{HHK} \qquad\quad \text{LK} \qquad\quad\;\; \text{HK}$$

The boiling point ranking is exactly the same as that of type I$_r$, but again, the "neat" operation is not likely. The reason is the

large relative volatility between the two reactants, and in fact, the normal boiling temperature difference is about 270 °C at atmospheric pressure. Figure 3 also shows two possible "excess reactant" designs. The first configuration is placing the reactive zone at the upper section of a reactive distillation column, flowsheet A in Figure 3, where the light reactant (methanol) is introduced to the lower end of the reactive zone while the heavy reactant (adipic acid) is fed from the column top. With light reactant in excess, the unreacted methanol is withdrawn from the top and recycled back to the RD column. The other alternative is to place the reactive zone in the lower section of
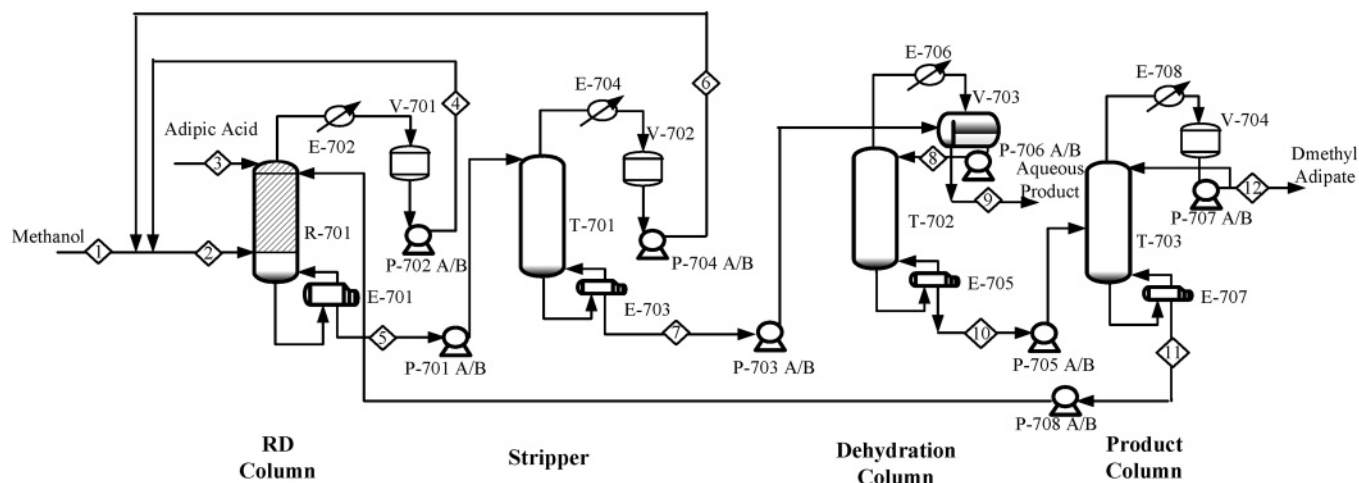
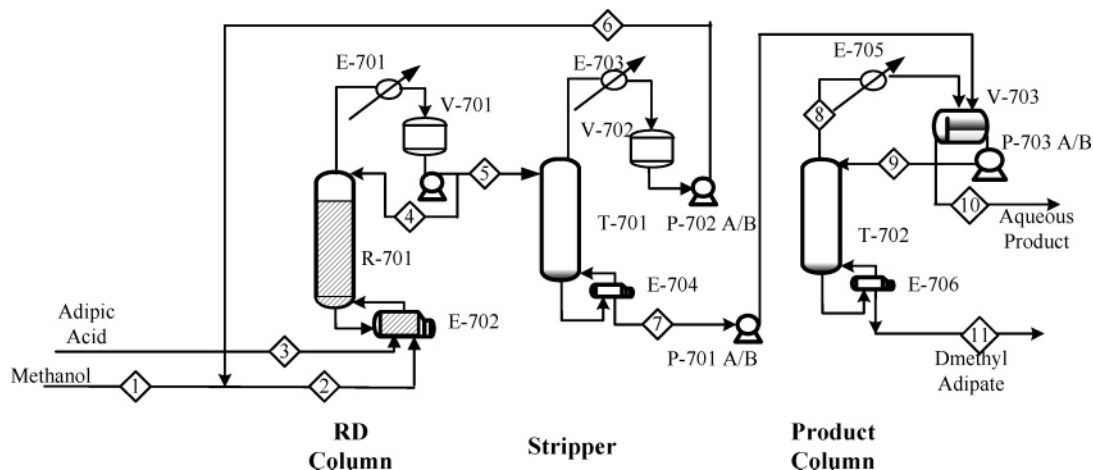**Figure 4.** Flowsheet A for dimethyl adipate production.

Figure 5. Flowsheet B for dimethyl adipate production.

a RD column, flowsheet B in Figure 3. Both reactants are fed into the column base, and the excess reactant (methanol) as well as products are removed from the overhead of the column. Note that there is no outlet at the bottom, and the configuration is quite similar to that for ethyl acetate production,[8] except for "excess" reactant design.

4.2. Complete Flowsheet. Because of the "excess" reactant design and multiple product nature, recycle column and product columns are necessary to complete the design of the entire plant. In this section, two flowsheets are devised for the production of high purity diester. As will be explained later, the placement of the reactant zone and the location for the withdrawal of the products result in different selectivities for these two flowsheets. Thus, the design for subsequent separation sections will be different.

4.2.1. Flowsheet A. Flowsheet A (FSA) is based on the RD column where the reactive zone is placed at the top (Figure 3). Because the intermediate product (MMA) is heavier than the main product (DMA), the selectivity is a little greater than 98%, e.g., 98.6%. Thus, MMA has to be recovered and recycled back to the RD. Figure 4 shows the complete process flowsheet. Because the light reactant (methanol) is much lighter than the product, the reactive distillation column is configured as a stripper, i.e., no condenser, and the lights, mostly methanol with some water, go out from the top of the reactive stripper. The overhead vapor, stream 4, is made of 80% methanol and 20% water, which is recycled and mixed with the fresh feed (stream 2) and then is fed into the lower section of the reactive zone. Because the limiting reactant, adipic acid, is near a complete

conversion, the bottoms flow, stream 5, of the reactive stripper is made of excess lights (MeOH and water) and heavy product and byproduct (DMA and MMA). In the separation section, a stripper (Figure 4, T-701) is used to prevent methanol leaving the system, and the overhead stream (stream 6) of the stripper is also recycled back to the reactive stripper. Thus, the major components in the stripper bottoms flow, stream 7, are water and DMA with a small amount of MMA. Because a tie line connects to the pure water node for the water–DMA pair (Figure 2), this stream is fed into the overhead decanter (Figure 2, V-703) of a dehydration column (Figure 4, V-703). Water is removed from the decanter while the organic phase is recycled back to the dehydration column, and the bottoms flow consists of mostly MMA and DMA. Finally, a product column (Figure 4, T-703) separates these two esters. High purity DMA is withdrawn from the top while the byproduct, MMA, is recycled back to the top reactive tray of the reactive stripper.

4.2.2. Flowsheet B. Flowsheet B (FSB) is based on the configuration where the reactive zone is placed at the lower section of the column and all the products and excess reactant are taken out from the column top. Unlike that in flowsheet A, the heavier intermediate product (MMA) is trapped in the reactive zone while the relatively light product (DMA) leaves the column with a trace amount of MMA. Thus, the selectivity is near 100%. Figure 5 shows the entire plant of the flowsheet B. The distillate (stream 5) of the RD is fed into the methanol recovery separator, a stripper (Figure 5, T-701), where most of the excess methanol is recovered. The bottom of the stripper (stream 7) is then fed into the decanter of the product column

Table 1. Results of Steady-State Designs of DMA System (Two Flowsheets) and DMG System

case	DMA (FSA)	DMA(FSB) (DMA)	DMG
total no. of trays including the reboiler in RD column	75	21	21
no. of trays in stripping section (N_S)	5	0	0
no. of trays in reactive section (N_{rxn})	70	13	12
no. of trays in rectifying section (N_R)	0	8	9
reactive tray	5−75	0−13	0−11
RD column diameter (m)	1.156	1.141	0.72
RD column reboiler duty (kW)	2479.85	2198.69	716.62
total no. of trays including the reboiler in stripper (N_{STR})	11	14	
stripper diameter (m)	0.83	0.912	
stripper reboiler duty (kW)	1185.31	1505.4	
total no. of trays including the reboiler in dehydration column (N_{DHC})	4		
dehydration column diameter (m)	0.576		
dehydration column reboiler duty (kW)	268.59		
total no. of trays including the reboiler in methanol recovery column (N_{MRC})			22
feed tray of methanol recovery column			15
methanol recovery column diameter (m)			0.611
methanol recovery column reboiler duty (kW)			746.73
total no. of trays including the reboiler in product column	21	3	3
product column diameter (m)	0.51	0.202	0.297
product column reboiler duty (kW)	200.63	183.48	212.91
decanter duty (kW)	−67.69	−62.45	−73.64
adipic acid feed tray	75	0	
glutaric acid feed tray			0
methanol feed tray	5	0	0
(total capital cost)/3($1000)	632.33	392.04	275.38
RD column	395.3	201.77	112.3
stripper or methanol recovery column	129.86	156.92	119.2
dehydration column (include decanter)	49.42		
product column (include decanter)	57.75	33.35	43.88
total operating cost ($1000/year)	430.784	495.805	134.0
catalyst cost	82.8	48.5	4.6
energy cost	347.984	447.305	129.4
TAC ($1000/year) (10 kmol/hr)	1063.114	887.845	409.38

(Figure 5, T-702) with less than 0.1% of methanol as impurity. Water (stream 10) is withdrawn from the decanter as a result of a significant two-liquid zone between water and DMA. High purity DMA is obtained from the column base (stream 11) because of easy separation between these two components. It is clear that the difference between flowsheet A and B lies in the fact that flowsheet B possesses a much better selectivity, as a result of the placement of the reactive zone. Therefore, compared with FSA, this flowsheet requires one fewercolumn.

4.3. Design Procedure. Once the conceptual design is completed, a systematic procedure is devised to achieve an improved design to reduce the TAC. The main design parameters for these two flowsheets are tray numbers of individual columns. Flowsheet A consists of a reactive stripper with an upper section reactive section ($N_{rxn,A}$) and a stripping separation section ($N_{S,A}$), a stripper ($N_{STR,A}$), a dehydration column (N_{DHC}), and a product column ($N_{PROD,A}$). Similarly, flowsheet B consists of a reactive distillation column with a lower reactive zone ($N_{rxn,B}$) and a rectifying section ($N_{R,B}$), a stripper ($N_{STR,B}$), and a product column ($N_{PROD,B}$). We assume the production rate of DMA is 10 kmol/h with a product purity of 99 mol %. The fresh feed flow rates of both reactants are set according to the stoichiometric balance ($FF_{MeOH} = 2FF_{AA}$), but methanol is in excess after combining the fresh feed with the recycle flow (stream 2 in Figures 4 and 5). For clarity, we define a parameter,

feed ratio, as the ratio of pure methanol and pure acid, denoted as $F_R = F_{MeOH}/FF_{AA}$ hereafter. So, the following variables can be adjusted to meet design specifications: the heat inputs of four columns and the feed ratio ($F_{R,A}$) in FSA, the reflux ratio (RR) of the RD, heat inputs of three columns, and the feed ratio ($F_{R,B}$) in FSB. Here, the reflux ratio of the RD in FSB is kept constant in order to prevent the column from violating the temperature constraint for the catalyst. The thermal stability of commercial ion-exchange resin is 190 °C for the ion-exchange resin (Amberlyst 70). Increasing the reflux ratio (RR) of the column top causes the heavy key components' return; also, the temperature in the RD column will increase. Thus, the manipulated variable RR will be set to a proper value to prevent the column temperature from getting too high. Specifications for these two flowsheets (FSA and FSB) are the following: (I) Conversion of limiting reactant is greater or equal to 99%. (II) The selectivity for the FSA should be greater than 98% and nearly 100% for the FSB. In terms of composition, the outlet concentration (from RD) of MMA is less than 1 mol % for the FSA (stream 5 in Figure 4) and 1 ppm for the FSB (stream 5 in Figure 5). (III) Methanol in the stripper bottoms is kept below 1 mol % (stream 7 in Figures 4 and 5). (IV) The water impurity in the bottoms of the dehydration column, FSA, is less than 1 mol % (stream 10 of Figure 4).

In flowsheet A, the heavy components (AA, MMA, DMA) tend to go out from the bottoms of the reactive stripper, and the purpose of the first two specifications (I and II) is to set a limit on undesired components in the separation section. Note that the different requirements on MMA in the second specification is due to the intrinsic property of boiling points. Again, even if we react away all the acid, the MMA becomes the heaviest component, and it can be produced using flowsheet A, without any specification on its concentration. Flowsheet B, on the other hand, gives an improved selectivity, if DMA is the major product. For a given production rate and product specifications, the following steps are adopted to obtain a near optimal design: (1) Guess the tray numbers in stripper in FSA ($N_{STR,A}$) and FSB ($N_{STR,B}$). (2) Guess the tray numbers of RD in stripping section in FSA ($N_{S,A}$) and rectifying section in FSB ($N_{R,B}$). (3) Guess the number of reactive trays ($N_{rxn,A}$ and $N_{rxn,B}$). (4) Change the RD heat input, $F_{R,A}$, and stripper heat input in FSA to meet specifications I, II, and III, respectively. Similarly, change the stripper heat input and $F_{R,B}$ in FSB to meet specifications II and III, respectively. (5) Go back to step 3 and change $N_{rxn,A}$ and $N_{rxn,B}$ until the TAC is minimized. (6) Go back to step 2 and change $N_{S,A}$ and $N_{r,B}$ until the TAC is minimized. (7) Go back to step 1 and change $N_{STR,A}$ and $N_{STR,B}$ until the TAC is minimized. (8) Use heat input of the dehydration column to meet specification IV (for FSA) and change N_{DHC} until the TAC is minimized. (9) Use heat inputs of the product column to meet the product specification, and change $N_{PROD,A}$ and $N_{PROD,B}$ until the TAC is minimized.

The TAC used to evaluate for the resultant design can be expressed as

$$TAC = \text{operating cost} + \frac{\text{capital cost}}{\text{payback year}}$$

Here, the operating cost includes the costs of steam, cooling water, and catalyst, and capital cost covers the cost of columns,
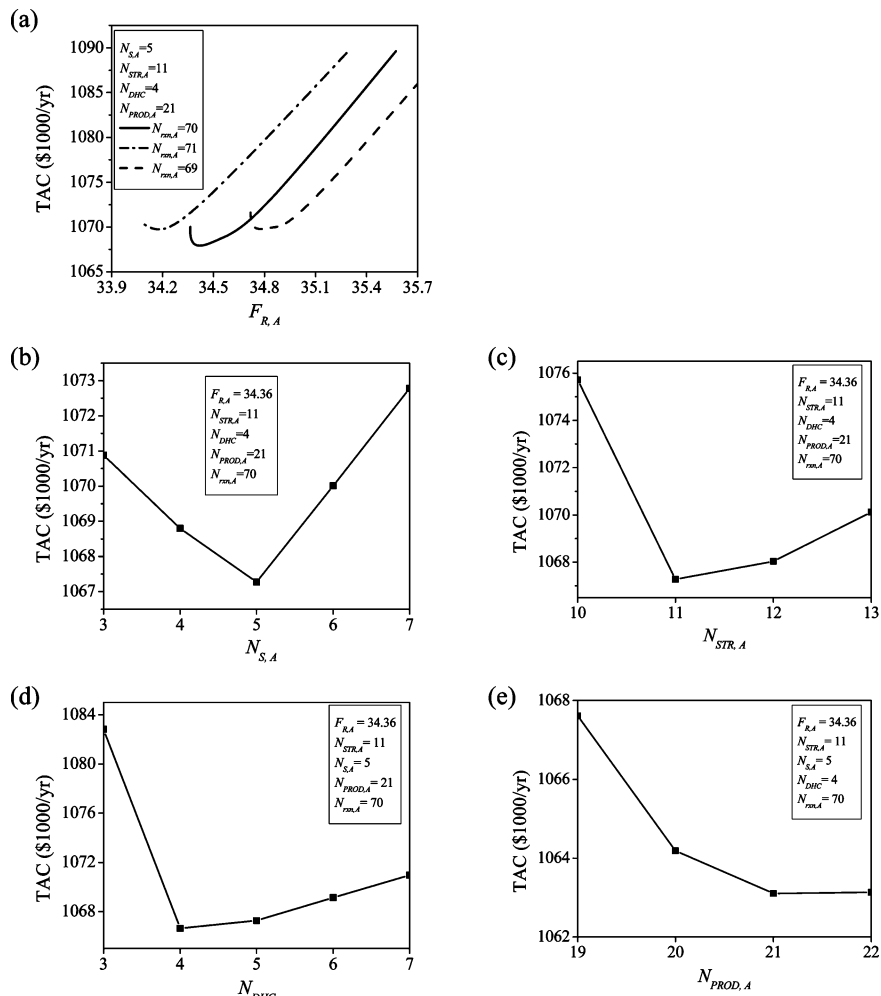
Figure 6. Effects of design variables on total annual cost for flowsheet A: (a) recycle ratio and number of reactive trays, (b) number of trays in the stripping section of the reactive stripper, (c) number of trays in the methanol recovery stripper, (d) number of trays in the dehydration column, and (e) number of trays in the product column.

Table 2. Stream Table of Flowsheet A for Adipic Acid Esterification

stream number	1	2	3	4	5	6	7	8	9	10	11	12
flow (kmol/h)	20.0	394.5	10.0	250.47	154.87	124.1	30.76	15.76	20.04	10.72	0.75	9.96
temperature (K)	356.4	357.6	453.15	339.9	356.3	339.9	369.8	318.1	318.1	511.4	538.8	509.0
pressure (atm)	2.0	1.56	2.0	1.0	1.56	1.01	1.10	1.0	1.0	1.01	1.06	1.0
AA (mol frac)	0	0.0001	1	0.0002	0.0006	0	0.0032	0.0050	0.0010	0.0074	0.1059	730 ppb*
MeOH	1	0.8711	0	0.8584	0.7029	0.8758	0.0050	0.0084	0.0076	0	0	0
MMA	0	0.0005	0	0.0007	0.0050	8 ppb	0.0251	0.0488	0.0003	0.0717	0.8841	0.0099
water	0	0.1237	0	0.1338	0.2271	0.1234	0.6453	0.2974	0.9904	0	0	0
DMA	0	0.0045	0	0.0068	0.0643	0.0007	0.3212	0.6402	0.0006	0.9207	0.0099	0.9900

*Parts per billion.

Table 3. Stream Table of the Flowsheet B for Adipic Acid Esterification

stream number	1	2	3	4	5	6	7	8	9	10	11
flow (kmol/h)	20.0	169.14	10.0	24.42	179.13	149.14	29.98	3.58	13.6	20.0	9.99
temperature (K)	356.4	342.6	453.15	413.8	342.8	339.4	369.3	370.0	318.1	318.1	465.1
pressure (atm)	2.0	1.2	2.0	1.1	1.0	1.0	1.10	1.1	1.0	1.00	1.1
AA (mol frac)	0	0	1	0	0	0	0	0	0	0	0
MeOH	1	0.9047	0	0.7426	0.7426	0.8919	99 ppm	0.0004	10 ppm	0.0015	43 ppb**
MMA	0	0	0	2 ppm*	2 pm	0	10 ppb	0	21 ppb	2 ppb	16 ppb
water	0	0.0948	0	0.2011	0.2011	0.1075	0.6667	0.9922	0.2692	0.9950	0.0096
DMA	0	0.0005	0	0.0562	0.0562	0.0005	0.3333	0.0077	0.7307	0.0048	0.9903

*Parts per million. **Parts per billion.

trays, exchangers, and reboilers. A payback year of 3 is used here.

5. Results and Discussion

The results of the steady-state design of these two flowsheets are given in Table 1. Tables 2 and 3 give the stream tables.

Because both flowsheets are quite similar, here we show the figure of optimization in FSA. Figure 6 shows the different variables affect the TAC in FSA. The numbers of trays in the separation section of different columns have little impact on TAC values. Figure 6a shows that $F_{R,A}$ has the greatest impact on TAC. Although the different feed ratio ($F_{R,A}$) values could meet the same specification, we always find the lowest TAC
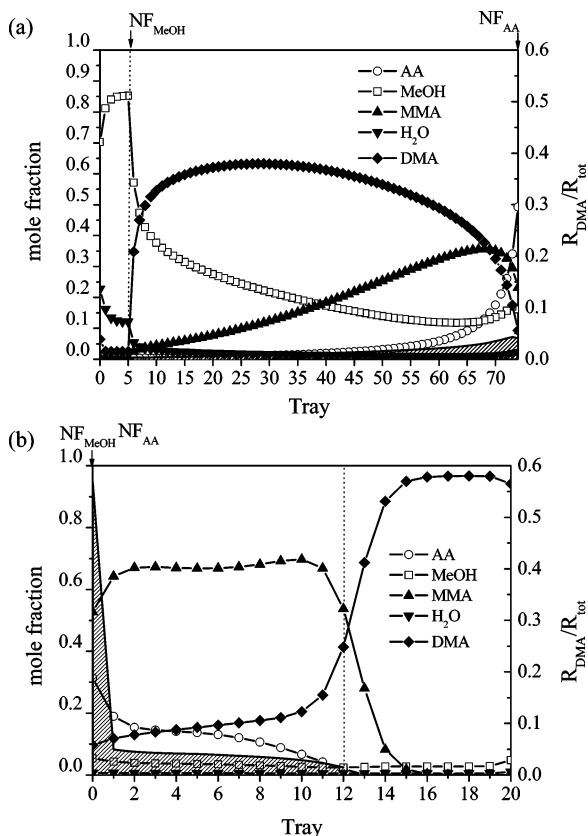
Figure 7. Composition profiles and fraction of total conversion (shaded area) in the reactive distillation column for flowsheet (a) A and (b) B.

Figure 8. (a) TAC comparison for two different flowsheets and (b) cost breakdown for two different flowsheets.

for a specific value of $F_{R,A}$ (Figure 6a) using different numbers of reactive trays. The tradeoff comes from the competing costs for the reactive stripper and methanol recovery column. A larger recycle flow will increase the energy demand in the methanol recovery column while facilitating the reaction (as the result of higher light reactant concentration). The same observation also applies to FSB where a proper feed ratio is important to the design. The difference comes from the fact that flowsheet B has a greater advantage in terms of placement of the reactive zone, the relative position of product withdrawal, and the amount of catalyst loading. Thus, $F_{R,B}$ is less than half of the value of $F_{R,A}$. Figure 7 shows concentration profiles and the fraction of total conversion (to the major product) in the RD column for both flowsheets. The area with gray hatching shows the fraction of the total conversion that takes place on each tray. In Figure 7b, almost 50% of reaction takes place in the column base for FSB; the remaining 50% of reaction takes place in the column (note the tray numbers are counted from the bottom). Figure 7a shows that although the reaction occurs anywhere in the entire reactive section, the bulk reaction still takes place in the upper section, where the concentration of the limiting reactant (adipic acid) is higher. Detailed comparisons of the TACs are given in Figure 8. The results show that the TAC of flowsheet A is 20% higher than that of flowsheet B, in which the capital cost of FSA is 60% higher and the energy cost is 29% lower as compared to those of FSB. Figure 8b reveals the costs of different process units for these two flowsheets.

6. Extension to Dimethyl Glutarate

Because of economic advantages, flowsheet B is adopted here for the two-stage esterification systems that have similar properties. In this section, we extend the process design to the production of dimethyl glutarate (DMG). The esterification of
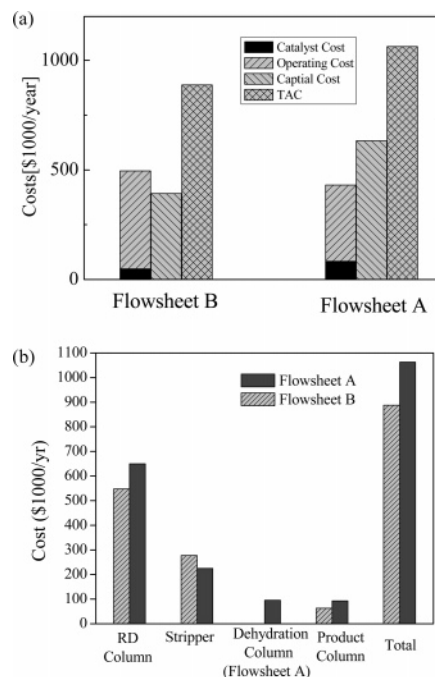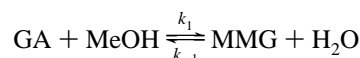
glutaric acid (GA) and methanol (MeOH) proceeds by a two-stage reversible reaction with glutaric acid monomethyl ester (monomethyl glutarate, MMG) as an intermediate:

$$GA + MeOH \underset{k_{-1}}{\overset{k_1}{\rightleftharpoons}} MMG + H_2O$$

$$MMG + MeOH \underset{k_{-2}}{\overset{k_2}{\rightleftharpoons}} DMG + H_2O \tag{8}$$

Similar to the adipic acid esterification, the reaction rates can also be described by eq 2. The rate constants shown below have a unit of cm^6/g catalyst/min/mol, taken from the work of Tsai.[20]
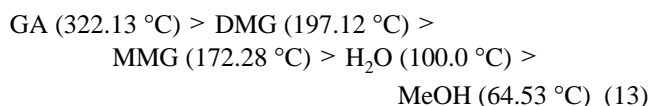
$$k_1 = 3.346 \times 10^7 \exp\left(\frac{-4417.4}{T}\right) \tag{9}$$

$$k_{-1} = 6.416 \times 10^3 \exp\left(\frac{-84.5}{T}\right) \tag{10}$$

$$k_2 = 3.487 \times 10^5 \exp\left(\frac{-2042.2}{T}\right) \tag{11}$$

$$k_{-2} = 2.024 \times 10^6 \exp\left(\frac{-4201.1}{T}\right) \tag{12}$$

Again, the UNIFAC method was used to estimate all the NRTL-HOC parameters. On the basis of the group contribution method and Aspen built-in data bank, the normal boiling points are ranked below in the descending order

GA (322.13 °C) > DMG (197.12 °C) >
MMG (172.28 °C) > H$_2$O (100.0 °C) >
MeOH (64.53 °C) (13)

This is a little different from the adipic acid system, because the boiling point of the major product, DMG, is higher than that of the byproduct, MMG. Similar to the adipic acid system, the two reactants still have the highest and lowest boiling points.
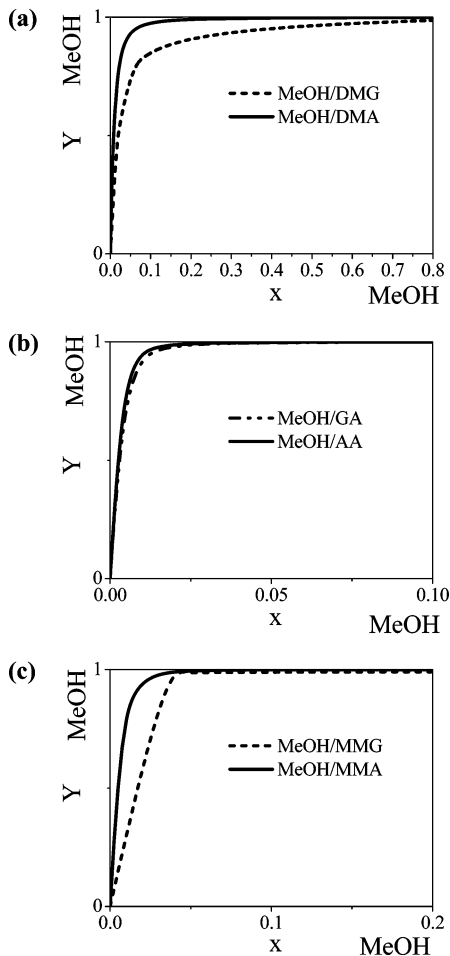
Figure 9. Comparisions with VLE diagrams for (a) dimethyl adipate and dimethyl glutarate + methanol, (b) dimethyl adipate and dimethyl glutarate + methanol, and (c) monomethyl adipate and monomethyl glutarate + methanol.

Before getting into the flowsheet generation, we examine the difference between the glutaric acid and adipic acid systems. The boiling point temperature difference between the excess reactant, methanol, and the product is 172 °C for the adipic acid system and 132 °C for the glutaric acid system. This implies that it is more difficult to separate methanol from the products for the glutaric system as compared to the adipic acid system (Figure 9a) while the boiling point difference is negligible for

these two systems (Figure 9b). In terms of process design, that means that a distillation column will be more appropriate as compared to the stripper (Figure 5, T-701) for the glutaric system. Thus, a distillation column is used instead of a stripper (Figure 10, T-701).

The design steps are quite similar to those of DMA systems except for the methanol recovery column. The reflux ratio of the distillation column is used to prevent the product, DMG, from recycling back to the RD column, and the specification for the impurity is 1%. After a sequential search, the best value of the feed ratio (F_{MeOH}/F_{acid}) for TAC minimization is found to be 6.1 (Figure 11a). Figure 11b shows the TAC when the number of reactive trays is varied. In this process, we also consider the feed tray location of the recovery column (NF_{RC}). Figure 11c shows the effect of a different number of trays in the rectifying section, and Figure 11d shows the TAC for the product column settings. The result of the steady-state design of the DMG system is given in the fourth column of Table 2. Table 4 lists all the stream information. Figure 12 shows the composition profile and the fraction of total conversion of the DMG system.

It is interesting to note that the TAC of the glutaric acid system is less than half of that of the adipic acid system. The energy cost ($447000 versus $129000), especially in the reactive distillation reboiler duty (2199 and 717 kW), accounts for 75% of the difference, and the remaining 25% comes from the capital cost ($392000 versus $275000). The reason for that is the significantly different rate constant. For example, rate constants at 180 °C for these two systems are

$$\text{adipic acid: } k_1/k_{-1}/k_2/k_{-2} = 692/695/191/74$$

$$\text{glutaric acid: } k_1/k_{-1}/k_2/k_{-2} = 1954/5325/3848/3670$$

The forward reaction rate for the glutaric acid esterification is 3−20 times faster than that of the adipic acid system, and moreover, the second stage reaction of the gultaric acid system is twice as fast as the first stage reaction. Therefore, a much lower monoester concentration is observed in the DMG system (Figure 12) as compared to that of the DMA system (Figure 7b). It should be noticed here that the equilibrium constants ($K_{1,eq}$ and $K_{2,eq}$) for the adipic acid are 2−3 times larger than those of the glutaric acid system, but this difference does not impose difficulty for reactive distillation with multistage reaction/separation capability. Despite the fact that the boiling point ranking of the adipic acid is favorable for improved selectivity
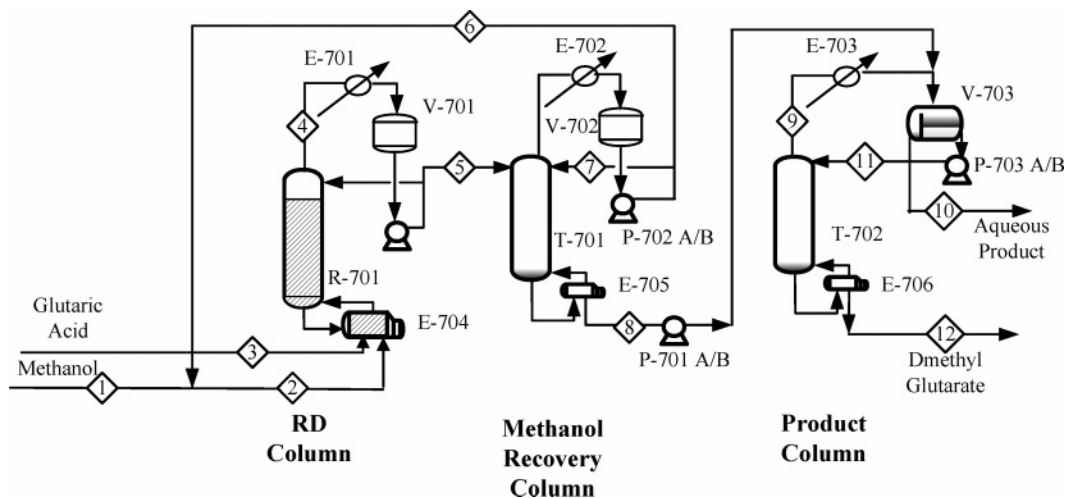

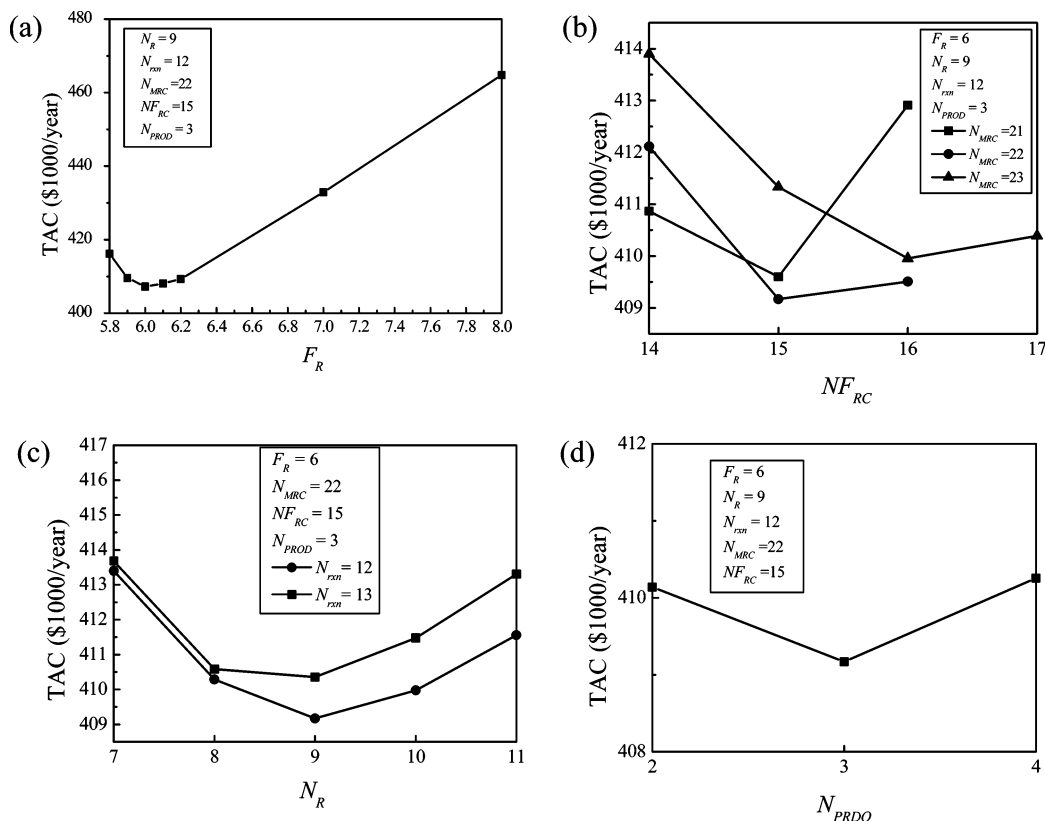**Figure 10.** Flowsheet for dimethyl glutarate production.

Figure 11. Effects of design variables on total annual cost: (a) recycle ratio, (b) feed tray location and number of trays in the methanol recovery column, (c) number of trays in the rectifying section and number of reactive trays of the reactive distillation column, and (d) number of trays in the product column.

Table 4. Stream Table for Glutaric Acid Esterification

stream number	1	2	3	4	5	6	7	8	9	10	11	12
flow (kmol/h)	20.0	63.44	10.0	7.77	73.44	43.44	31.28	30.0	7.75	19.97	17.78	10.03
temperature (K)	356.4	347.8	351.2	352.8	356.3	343.6	343.6	376.3	372.3	323.15	323.15	463.7
pressure (atm)	2.0	1.5	2.0	1.2	1.56	1.2	1.2	1.3	1.1	1.0	1.0	1.1
AA (mol frac)	0	0	1	0	0	0	0	0	0	0	0	0
MeOH	1	0.9455	0	0.5445	0.5445	0.9205	0.9205	100 ppm	0.0006	0.0001	0.0003	6 ppm
MMA	0	0	0	0	0	0	0	2 ppb	0	0	4 ppb	7 ppb
water	0	0.0543	0	0.3192	0.3192	0.0793	0.0793	0.6667	0.9311	0.9963	0.4159	0.0099
DMA	0	688 ppm*	0	0.1362	0.1362	99 ppm	99 ppm	0.3333	0.0629	0.0035	0.5838	0.9900

* Parts per million.

(compared to glutaric system), the reaction kinetics dominates the outcomes of process design, as the result of the order of magnitude difference. The comparison made here illustrates the importance of absolute rate constant to the cost of reactive distillation systems.
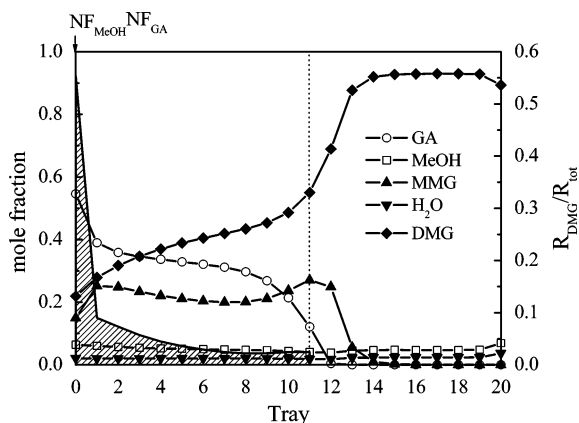

Figure 12. Composition profiles and fraction of total conversion (shaded area) in the reactive distillation column for gultaric acid esterification.

7. Conclusion

This paper proposes conceptual designs for the reactive distillation processes for adipic acid esterification, a two-stage reversible reaction. Provided with experimental data on vapor pressure and UNIFAC method estimated NRTL parameters, the NTRL-HOC model provides a reasonably good description of phase equilibria. Two possible process flowsheets are generated at the conceptual design level. A systematic design procedure is presented to improve the quantitative design based on the total annual cost (TAC). Similarities and differences of these two flowsheets are explored, and explanations of the different economical potentials are given. Results show that both plant-wide flowsheets need a large recycle ratio for the light reactant and high purity diesters can be produced. Because of unfavorable boiling point ranking (the reactants being the lightest and heaviest) and the "excess-reactant" operation, relatively, the TACs are much higher as compared to the cases for single-stage acetic acid esterification.[8] The approach can be extended to the glutaric acid esterification with little modification. Appendix

Model parameters used in vapor pressure, VLE, and VLLE computation for adipic acid and glutaric esterification systems appear in Tables 5–8.

Table 5. Extended Antoine Equation[a] Parameters for MMA, DMA, MMG, and DMG

component	C_1	C_2	C_3	C_4	C_5
MMA	−4503.023	103889.81	0.000	1.314	794.908
DMA	1139.710	−39383.491	0.000	0.285	−192.449
MMG	−8555.6	1.827×10^6	0.000	10.00	0.000
DMG	$−5.505 \times 10^5$	1.739×10^7	0.000	−128.16	93139.4

^{a} $\ln P$ (kPa) $= C_1 + C_2/(T \text{ (K)} + C_3) + C_4 T \text{ (K)} + C_5 \ln T \text{ (K)}$.

Table 6. NRTL[a] Binary Parameters in DMA System

	AA (1)/ MeOH (2)	AA (1)/ MMA (3)	AA (1)/ H$_2$O (4)	AA (1)/ DMA (5)	MeOH (2)/ MMA (3)
a_{ij}	0	0	0	0	0
a_{ji}	0	0	0	0	0
b_{ij} (K)	1414.087	−289.170	−385.150	−248.655	300.238
b_{ji} (K)	−753.363	545.044	1190.271	828.462	828.462
c_{ij}	0.300	0.300	0.300	0.300	0.300

	MeOH (2)/ H$_2$O (4)	MeOH (2)/ DMA (5)	MMA (3)/ H$_2$O (4)	MMA (3)/ DMA (5)	H$_2$O (4)/ DMA (5)
a_{ij}	−2.631	0	0	0	0
a_{ji}	4.868	0	0	0	0
b_{ij} (K)	838.593	687.142	48.026	−202.980	2029.890
b_{ji} (K)	−1347.527	−202.753	1698.559	309.407	347.370
c_{ij}	0.300	0.300	0.300	0.300	0.300

^{a} NRTL model:

$$\ln\gamma_i = \frac{\sum_{j=1}^{nc} \tau_{ji} G_{ji} x_j}{\sum_{k=1}^{nc} G_{ki} x_k} + \sum_{j=1}^{nc} \frac{x_j G_{ij}}{\sum_{k=1}^{nc} G_{kj} x_k} \left[\tau_{ij} - \frac{\sum_{k=1}^{nc} x_k \tau_{ki} G_{kj}}{\sum_{k=1}^{nc} G_{kj} x_k} \right]$$

$G_{ij} = \exp(-\alpha_{ij}\tau_{ij})$, $\tau_{ij} = a_{ij} + b_{ij}/T$, $\alpha_{ij} = c_{ij}$, $G_{ii} = 1$, and $\tau_{ii} = 0$.

Table 7. NRTL[a] Binary Parameters in DMG System

	GA (1)/ MeOH (2)	GA (1)/ MMG (3)	GA (1)/ H$_2$O (4)	GA (1)/ DMG (5)	MeOH (2)/ MMG (3)
a_{ij}	0	0	0	0	0
a_{ji}	0	0	0	0	0
b_{ij} (K)	1322.396	−381.653	−319.111	901.943	306.376
b_{ji} (K)	−708.714	1029.585	1010.599	−459.037	−17.346
c_{ij}	0.300	0.300	0.300	0.300	0.300

	MeOH (2)/ H$_2$O (4)	MeOH (2)/ DMG (5)	MMG (3)/ H$_2$O (4)	MMG (3)/ DMG (5)	H$_2$O (4)/ DMG (5)
a_{ij}	−2.631	0	0	0	0
a_{ji}	4.868	0	0	0	0
b_{ij} (K)	838.593	618.625	129.261	422.576	1698.556
b_{ji} (K)	−1347.527	−334.455	1423.055	−216.035	48.026
c_{ij}	0.300	0.300	0.300	0.300	0.300

^{a} NRTL model:

$$\ln\gamma_i = \frac{\sum_{j=1}^{nc} \tau_{ji} G_{ji} x_j}{\sum_{k=1}^{nc} G_{ki} x_k} + \sum_{j=1}^{nc} \frac{x_j G_{ij}}{\sum_{k=1}^{nc} G_{kj} x_k} \left[\tau_{ij} - \frac{\sum_{k=1}^{nc} x_k \tau_{ki} G_{kj}}{\sum_{k=1}^{nc} G_{kj} x_k} \right]$$

$G_{ij} = \exp(-\alpha_{ij}\tau_{ij})$, $\tau_{ij} = a_{ij} + b_{ij}/T$, $\alpha_{ij} = c_{ij}$, $G_{ii} = 1$, and $\tau_{ii} = 0$.

Table 8. NRTL[a] Binary Parameters in DMA System (Use for LLE Calculation)

	AA (1)/ MeOH (2)	AA (1)/ MMA (3)	AA (1)/ H$_2$O (4)	AA (1)/ DMA (5)	MeOH (2)/ MMA (3)
a_{ij}	0	0	0	0	0
a_{ji}	0	0	0	0	0
b_{ij} (K)	1414.087	−289.170	−385.150	−248.655	300.238
b_{ji} (K)	−753.363	545.044	1190.271	828.462	828.462
c_{ij}	0.300	0.300	0.300	0.300	0.300

	MeOH (2)/ H$_2$O (4)	MeOH (2)/ DMA (5)	MMA (3)/ H$_2$O (4)	MMA (3)/ DMA (5)	H$_2$O (4)/ DMA (5)
a_{ij}	−2.631	0.549	−1.562	0	4.039
a_{ji}	4.868	−2.988	11.329	0	−2.995
b_{ij} (K)	838.593	452.196	373.602	−540.931	218.692
b_{ji} (K)	−1347.527	−108.168	−2476.828	1416.366	1160.862
c_{ij}	0.300	0.300	0.665	0.300	0.2936

^{a} NRTL model:

$$\ln\gamma_i = \frac{\sum_{j=1}^{nc} \tau_{ji} G_{ji} x_j}{\sum_{k=1}^{nc} G_{ki} x_k} + \sum_{j=1}^{nc} \frac{x_j G_{ij}}{\sum_{k=1}^{nc} G_{kj} x_k} \left[\tau_{ij} - \frac{\sum_{k=1}^{nc} x_k \tau_{ki} G_{kj}}{\sum_{k=1}^{nc} G_{kj} x_k} \right]$$

$G_{ij} = \exp(-\alpha_{ij}\tau_{ij})$, $\tau_{ij} = a_{ij} + b_{ij}/T$, $\alpha_{ij} = c_{ij}$, $G_{ii} = 1$, and $\tau_{ii} = 0$.

Nomenclature

AA = adipic acid
C_i = concentration of component i
DBE = dibasic ester
DMA = dimethyl adipate
DMG = dimethyl glutarate
DMS = dimethyl succinate
F_{AA} = adipic acid flow rates
F_{MeOH} = methanol flow rates
FF_{AA} = adipic acid feed flow rates
FF_{MeOH} = methanol feed flow rates
F_R = feed ratio
FSA = flowsheet A
FSB = flowsheet B
GA = glutaric acid
HK = heavy key component
HHK = heavier than heavy key component
k = rate constant
K_{eq} = equilibrium constant
LK = light key component
LLK = lighter than light key component
MeOH = methanol
MMA = monomethyl adipate
MMG = monomethyl glutarate
MRC = methanol recovery column
N_{DHC} = number of trays in dehydration column
NF_{RC} = feed tray location of methanol recovery column
N_{PROD} = number of trays in product column
N_R = number of trays in rectifying section
N_{MRC} = number of trays in methanol recovery column
N_{rxn} = number of trays in reactive section
N_S = number of trays in the stripping section
N_{STR} = number of trays in stripper
RC = methanol recovery column
RDC = reactive distillation column
RR = reflux ratio
TAC = total annual cost

X_{aq} = liquid mole fraction in aqueous phase
X_{PROD} = liquid mole fraction in product stream

Acknowledgment

Literature Cited

(1) Doherty, M. F.; Malone, M. F. *Conceptual Design of Distillation Systems*; McGraw-Hill: New York, 2001.

(2) Sundmacher, K.; Kienle, A. *Reactive Distillation: Status and Future Directions*; Wiley: Weinheim, 2003.

(3) Taylor, R.; Krishna, R. Modelling Reactive Distillation. *Chem. Eng. Sci.* **2000**, *55*, 5183.

(4) Agreda, V. H.; Partin, L. R.; Heise, W. H. High Purity Methyl Acetate via Reactive Distillation. *Chem. Eng. Prog.* **1990**, *86*, 40.

(5) Kenig, E. Y.; Bader, H.; Gorak, A.; Bessling, B.; Adrian, T.; Schoenmakers, H. Investigation of Ethyl Acetate Reactive Distillation Process. *Chem. Eng. Sci.* **2001**, *56*, 6185.

(6) Hanika, J.; Kolena, J.; Smejkal, Q. Butyl Acetate via Reactive Distillation—Modelling and Experiment. *Chem. Eng. Sci.* **1999**, *54*, 5202.

(7) Gangadwala, J.; Kienle, A.; Stein, E.; Mahajani, S. Production of Butyl Acetate by Catalytic Distillation: Process Design Studies. *Ind. Eng. Chem. Res.* **2004**, *43*, 136.

(8) Tang, Y. T.; Chen, Y. W.; Huang, H. P.; Yu, C. C.; Hung, S. B.; Lee, M. J. Design of Reactive Distillations for Acetic Acid Esterification. *AIChE J.* **2005**, *51*, 1683.

(9) Jacobs, R.; Krishna, R. Multiple Solutions in Reactive Distillation for Methyl Tert-Butyl Ethers Synthesis. *Ind. Eng. Chem. Res.* **1993**, *32*, 1706.

(10) Sundmacher, K.; Hoffmann, U. Multiple Reactions in Catalytic Distillation Processes for the Production of the Fuel Oxygenates MTBE and TAME: Analysis by Rigorous Model and Experimental Validation. *Chem. Eng. Sci.* **1999**, *54*, 2839.

(11) Ung, S.; Doherty, M. F. Synthesis of Reactive Distillation Systems with Multiple Equilibrium Chemical Reactions. *Ind. Eng. Chem. Res.* **1995**, *34*, 2555.

(12) Ung, S.; Doherty, M. F. Vapor-Liquid Phase Equilibrium in Systems with Multiple Chemical Reactions. *Chem. Eng. Sci.* **1995**, *50*, 23.

(13) Luo, H. P.; Xiao, W. D. A Reactive Distillation Process for a Cascade and Azeotropic Reaction System: Carbonylation of Ethanol with Dimethyl Carbonate. *Chem. Eng. Sci.* **2001**, *56*, 403.

(14) Chan, K. W. Kinetic Behavior of Heterogeneous Esterification of Adipic Acid with Methanol. M.S. Thesis, National Taiwan University of Science and Technology, Taipei, Taiwan, 2004.

(15) Lee, M. J.; Lai, C. H.; Wang, Z. B.; Lin, H. M. Vapor−Liquid Equilibrium of Mixtures Containing Adipic Acid, Glutaric Acid, Dimethyl Adipate, Dimethyl Glutarate, Methanol, and Water. *J. Chem. Eng. Data* **2007**, *52*, 1291.

(16) Hayden, J. G.; O'Connell, J. P. A Generalized Method for Predicting Second Virial Coefficients. *Ind. Eng. Chem. Process Des. Dev.* **1975**, *14*, 209.

(17) Fredenslund, A.; Gmehling, J.; Rasmussen, P. *Vapor-Liquid Equilibria Using UNIFAC: A Group-Contribution Method*; Elsevier: Amsterdam, 1977.

(18) Hung, S. B.; Lin, H. M.; Yu, C. C.; Huang, H. P.; Lee, M. J. Liquid−Liquid Equilibria of Aqueous Mixtures Containing Selected Dibasic Esters and/or Methanol. *Fluid Phase Equilib.* **2006**, *248*, 174.

(19) Tung, S. J.; Yu, C. C. Effects of Relative Volatility Ranking to the Design of Reactive Distillation. *AIChE J.* **2007**, *53*, 1278.

(20) Tsai, Y. T. Kinetic Behavior of Heterogeneous Esterification of Glutaric Acid with Methanol. M.S. Thesis, National Taiwan University of Science and Technology, Taipei, Taiwan, 2005.